Bioorganic & Medicinal Chemistry 17 (2009) 1831–1836

Contents lists available at ScienceDirect

Bioorganic & Medicinal Chemistry

journal homepage: www.elsevier.com/locate/bmc

GlcNAc-Thiazoline conformations

Spencer Knapp [a,*], David Fash [a], Mohannad Abdo [a], Thomas J. Emge [a], Paul R. Rablen [b,*]

[a] Department of Chemistry and Chemical Biology, Rutgers The State University of New Jersey, 610 Taylor Road., Piscataway, NJ 08854, USA
[b] Department of Chemistry and Biochemistry, Swarthmore College, 500 College Avenue, Swarthmore, PA 19081, USA

ARTICLE INFO

Article history:
Received 17 December 2008
Revised 22 January 2009
Accepted 24 January 2009
Available online 3 February 2009

Keywords:
Enzyme inhibitors
NOE
Ab initio calculations
Mitsunobu reaction

ABSTRACT

The title compound, a powerful inhibitor of retaining *N*-acetylhexosaminidases, can move freely among three pyranose solution conformations of similar energy—two twist boats and the $^4C_1$ chair—as revealed by NMR, calculational, and crystallographic studies. It binds in the enzyme active site only in the *pseudo*-$^4C_1$ conformation, however, in which it most closely resembles the hypothetical bound substrate transition state, a ^4E sofa that is approximately trigonal bipyramidal at the anomeric carbon.

1. Introduction

A number of retaining *N*-acetylhexosaminidases, including the bacterial enzyme from *Streptomyces plicatus* (SpHex), and the human enzymes *O*-GlcNAcase (OGA) and HexA and HexB, use a two step mechanism that proceeds by way of a non-covalently bound oxazoline intermediate **A** → **C** (Fig. 1).[1] Participation of the substrate amide carbonyl in a transition state **B** that features a *pseudo*-sofa ^4E conformation of the pyranose ring and a roughly trigonal bipyramidal anomeric carbon allows charge distribution throughout the assembly and avoids the build-up of high-energy oxocarbenium character at C-1 such as might occur in solution hydrolysis. The GlcNAc-thiazoline **1** (Fig. 2) is a powerful inhibitor of these enzymes: respective K_i for **1** = 20 μM versus SpHex,[2,3] 70 nM versus human Hex,[4] and 70 nM versus OGA.[4] Recently, Vocadlo has shown that **1** is a true transition state mimic for OGA; that is, **1** and its homologues display excellent correlation of free energy of activation calculated from enzymatic substrate hydrolysis relative to $\Delta G^{\ddagger}$ for inhibitor binding.[5] Furthermore, protein crystallographic studies reveal that **1** binds in enzyme active sites[2,5–9] in the *pseudo*-chair ($^4C_1$) conformation **E**. This suggests that **E** (rather than the twist boat **D**, which resembles the bound substrate **A**) is the specific conformation that most closely matches the transition state **B**.

The details of the relationship between inhibitor conformation and binding are important for understanding the interactions of substrate with enzyme, and for the design of new inhibitors.[10] With regard to the latter, there is a tradeoff between anchoring an inhibitor in a good conformation for binding, or allowing conformational flexibility so that a conformation with somewhat higher energy in solution, but which might bind in the active site more tightly, is accessible. An additional aspect is that, confronted with

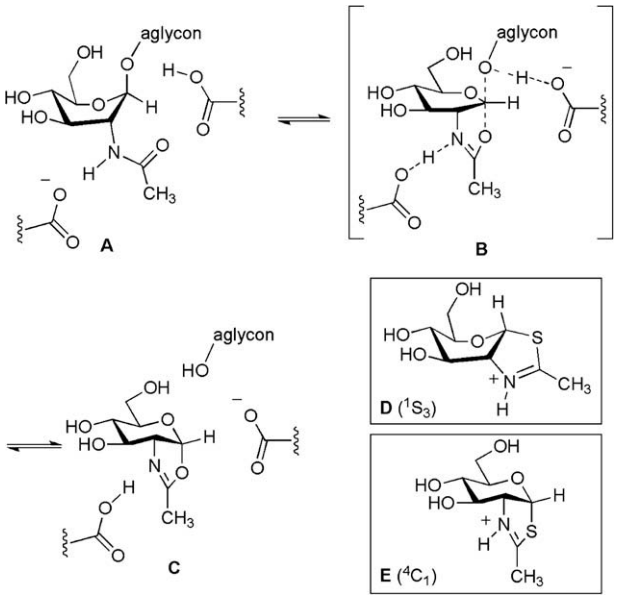

Figure 1. The *N*-acetylhexosaminidase mechanism with substrate participation and oxazolinium intermediate (**A** → **[B]** → **C**), and the protonated GlcNAc-thiazoline inhibitor in two conformations (**D** and **E**).

* Corresponding authors. Tel.: +1 732 445 2627; fax: +1 732 445 5312 (S. Knapp).. *E-mail address:* spencer.knapp@rutgers.edu (S. Knapp).

0968-0896/$ - see front matter © 2009 Elsevier Ltd. All rights reserved.
doi:10.1016/j.bmc.2009.01.066

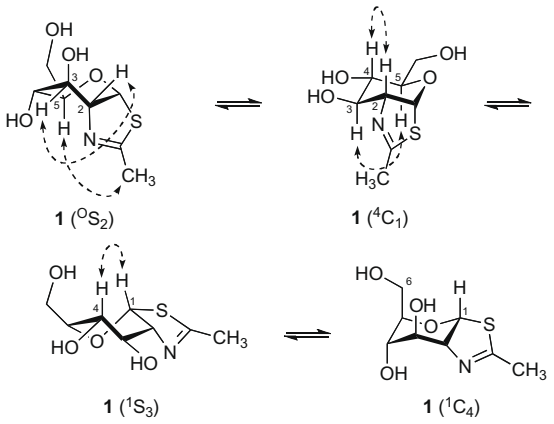

Figure 2. Four GlcNAc-thiazoline (**1**) conformations. Dashed arrows represent diagnostic NOE signals observed.

the ability of some target microorganisms to mutate, and thus to modify the details of an enzyme active site, flexible molecules retain a chance to inhibit the mutant forms as well.[11]

In this paper, we examine the conformational properties of **1** and its derivatives in solution (by NOE and vicinal proton coupling constant measurements), in the crystal (by single crystal X-ray studies of a derivative), and in the gas phase (by hybrid density functional electronic structure calculations). A coherent picture emerges: we provide evidence that these pyranose-fused thiazolines can shift freely among several conformations, and that little energetic sacrifice is required for **1** to achieve the pyranose $^{4}C_1$ *pseudo*-chair conformation required for binding in the enzyme active site.

2. Results and discussion

2.1. Calculation and comparison of NMR parameters for GlcNAc-thiazoline conformations

In D_2O or MeOH-d_4 solution, and at concentrations ranging from 12–115 mM, thiazoline **1** is *not* primarily in the pyranose $^{4}C_1$ *pseudo*-chair conformation (Fig. 2), as evidenced by the small vicinal proton coupling for H-2/H-3 and H-3/H-4 (pyranose numbering), nor is the major conformation $^{1}S_3$ by the same argument. Table 1 shows the observed proton and carbon chemical shifts for **1** along with calculated values for four pyranose conformations: $^{O}S_2$, $^{4}C_1$, $^{1}S_3$, and $^{1}C_4$. Table 2 shows the respective observed and calculated vicinal proton coupling constants. There is a good but not perfect match with the $^{O}S_2$ twist boat, which also happens to be the preferred conformation of the 3,4,6-tri-*O*-acetyl derivative (**2**) of **1** in deuteriochloroform solution, and of the 2,4-dinitrobenzenesulfonate salt (**3**) of **2** in the crystal.[12] The GalNAc-thiazoline **4**, also an inhibitor of retaining *N*-acetylhexosaminidases, exists in the $^{4}C_1$ pseudo-chair in solution, in the crystal, and presumably also in the enzyme active site.[13]

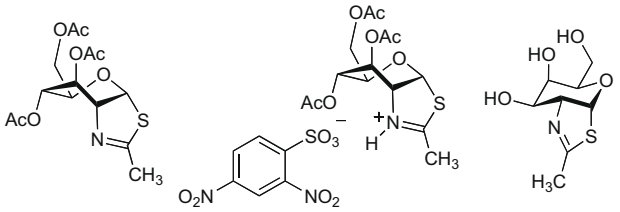

2.2. NOE measurements

Attempts to cool methanolic solutions of **1** to −78 °C in order to freeze out individual contributing conformations and to identify them by ^{1}H NMR spectroscopy were unsuccessful. However, NOE studies on **1** in methanol-d_4 solution revealed a number of proton–proton through-space contacts that can be attributed to one or more of the four conformations shown in Figure 2. The diagnostic H···H contacts for each conformation are also displayed in Figure 2 (dashed arrows). Table 3 summarizes the qualitative NOE enhancements observed upon irradiation at each of eight proton signals. The H-2/H-3 and H-5/Me NOEs are (among these four possibilities) uniquely due to the $^{O}S_2$ conformation, and the intensity of these signals indicates that this is indeed the major contributing conformation in methanol solution.[14] Additionally, the weaker NOEs observed for H-2/H-4 and H-3/H-5 can be uniquely attributed to the $^{4}C_1$ conformation, and this must be considered a minor contributing structure inasmuch as a blend of larger H-2/H-3 and H-3/H-4 vicinal proton coupling constants with those of $^{O}S_2$ is required by the data in Table 2. Furthermore, a very weak H-1/H-4 NOE is observed, and this is unique (again, among these four pos-

Table 1
Observed and calculated ^{1}H and ^{13}C chemical shifts for **1**[a]

Thiazoline **1** (obsd)	**1** ($^{O}S_2$, Calculated)	**1** ($^{4}C_1$, Calculated)	**1** ($^{1}S_3$, Calculated)	**1** ($^{1}C_4$, Calculated)
6.36 (H-1)	6.03	6.48	5.57	6.55
4.32 (H-2)	4.4	3.89	3.88	3.33
4.13 (H-3)	4.23	3.40	3.74	4.87
3.56 (H-4)	3.21	3.30	3.42	3.53
3.33 (H-5)	3.19	3.88	3.78	3.55
3.74 (H-6)	3.69	4.03	3.60	4.00
3.61 (H-6)	3.45	3.62	3.74	3.82
2.26 (Me)	2.28	2.16	2.24	2.28
	RMS abs err: 0.19	RMS abs err 0.39	RMS abs err: 0.39	RMS abs err: 0.46
90.92 (C-1)	94.14	99.55	88.61	90.08
80.64 (C-2)	79.32	76.48	86.89	80.29
74.31 (C-3)	70.37	76.32	74.73	69.10
71.48 (C-4)	70.39	67.11	68.75	69.05
76.43 (C-5)	78.33	73.79	81.37	80.55
63.65 (C-6)	63.05	60.89	59.09	64.84
171.04 (C=N)	177.61	176.97	172.96	178.35
20.79 (Me)	16.06	18.14	16.87	17.00
	RMS abs err: 3.51	RMS abs err: 4.63	RMS abs err: 3.81	RMS abs err: 3.88

[a] Chemical shifts in ppm.

Table 2
Observed and calculated vicinal ^{1}H coupling constants for **1**[a]

Vicinal *J*	**1** (Obsd)	**1** ($^{O}S_2$, Calculated)	**1** ($^4C_1$, Calculated)	**1** ($^1S_3$, Calculated)	**1** ($^1C_4$, Calculated)
H-1/H-2	7.2	6.8	7.0	6.4	3.7
H-2/H-3	4.2	4.0	7.1	6.5	1.9
H-3/H-4	3.8	1.6	7.4	8.5	2.5
H-4/H-5	9.2	5.8	7.6	6.6	1.3
H-5/H-6	2.4	3.0	2.9	3.1	1.1
H-5/H-6	6.4	8.1	8.0	9.1	4.3
H-6/H-6	12.0	11.1	10.9	11.0	12.2
H-2/Me	2.0				2.28
H-2/H-4	0.8				
		RMS error: 1.7	RMS error 2.0	RMS error: 2.5	RMS error: 3.4

[a] Coupling constants in hertz.

Table 3
Qualitative Individual NOEs for **1**[a,b]

Proton *hν*→	H-1	H-2	H-3	H-4	H-5	H-6	H-6'	CH_3
1	—	****	*	*	*		Overlaps	*
2	****	—	***	*			H-4	*
3	*	***	–	**	***			*
4	*	*	***	—		**		
5	*		***	**	—	***		**
6				**	***	—		
6′				**	***	***	—	
CH_3	*	*			*			—

[a] Observed for a MeOH-d_4 solution of **1** at 25 °C.
[b] Key: ****, strong NOE observed; ***, medium NOE; **, weak NOE; *, very weak NOE; (blank), no NOE; —, selfsame proton.

sibilities) to the $^1S_3$ conformation. Thus, a small contribution by the $^1S_3$ is indicated. The absence of an H-1/H-6 NOE suggests that the contribution of the $^1C_4$ conformation is negligible, although there is other evidence (see below) that even this conformation is attainable in solution.

2.3. Calculation of relative energies of GlcNAc-thiazoline conformations

Hybrid density functional electronic structure calculations were performed on the $^{O}S_2$, $^4C_1$, $^1S_3$, and $^1C_4$ conformations of **1** in order to obtain information about the relative energies and to correlate the NMR properties of these conformers. Geometry optimizations were carried out at the B3LYP/6-31G* level for each of the four conformations,[15] and B3LYP/6-311++G** single point calculations were additionally performed at the B3LYP/6-31G* optimized geometries; the results are summarized in Table 4. An intramolecular H-bond between the C-6 hydroxyl and the ring oxygen is indicated for the gas phase low energy conformations of the $^{O}S_2$, $^4C_1$, and $^1S_3$, between the C-4 hydroxyl and O-3 for $^4C_1$ and $^1S_3$, and between the C-6 hydroxyl and O-3 for $^1C_4$. These H-bonds would likely not be as significant in methanol solution. Despite the obvious differences between solution and gas phase analysis, the calculations offer a qualitative confirmation of the NOE evidence for the predominance of the $^{O}S_2$ and $^4C_1$ as the most stable conformations, and also support the view that the $^{O}S_2$, $^4C_1$, and $^1S_3$ conformations are close in energy (within 1–2 kcal/mol). The $^1C_4$ is considerably less stable than the other three.

Table 4
Calculated relative energies of the conformations of **1**

Conformation of **1**	B3LYP/6-31G* E_{rel} (kcal/mol)	B3LYP/6-311++G** E_{rel} (kcal/mol)
$^{O}S_2$	0.00	0.00
$^4C_1$	0.41	−0.84
$^1S_3$	2.20	0.84
$^1C_4$	2.62	3.70

2.4. X-ray crystallographic analysis

We sought to investigate the conformational properties of **1** in the solid phase in order to get realistic bond distances, angles, and other details. In contrast to the isomeric GalNAc-thiazoline **4**,[12] however, the parent GlcNAc-thiazoline **1** and its various salts did not crystallize. Although we were aware that O-substitution might influence the relative energies of the respective pyranose conformations, we resorted to chemical derivatization in order to obtain crystals for X-ray analysis. Treatment of **1** (Scheme 1) under Mitsunobu conditions {myristic acid [$CH_3(CH_2)_{12}CO_2H$], diisopropyl azodicarboxylate (DIAD), and triphenylphosphine} led to two crystalline thiazoline products: the 6-*O*-tetradecanoyl ester **5** (21%) and the tricyclic internal (3,6-anhydro) ether **6** (10%). Their structures were chemically confirmed by converting them to their respective acetates **7** and **8**. Furthermore, both **5** and **6** proved amenable to crystallographic analysis.

The tetradecanoate **5** crystallizes in a unit cell that contains two molecules in *different pyranose conformations hydrogen bonded to each other*: the $^4C_1$ and $^1S_3$ (Fig. 3). Both of these conformations had been also implicated as contributors by the calculations and by the NOE studies. The tetradecanoate chains are oriented in a pseudo-equatorial disposition with respect to the pyranose rings, and do not appear to interact strongly with the pyranose/thiazoline rings, although they stack with one another in adjacent molecules (see ORTEPs in Supplementary data). While crystal packing forces certainly play a role, one cannot escape the obvious conclusion that, since they co-occur, these two ring conformations must be of comparable energy. Interestingly, the most stable conformation of **1** and **5** in solution, namely $^{O}S_2$, does not appear in this crystal at all. This is likely the result of the *trans* disposition of N and HO(3), so that an intermolecular N···HO(3) hydrogen bond, which holds the dimers of the $^4C_1$ and $^1S_3$ together, cannot as easily form in the $^{O}S_2$ conformation. The crystal structure of **6** (Fig. 4) shows the expected 3,5-bridged $^1C_4$ conformation. The formation of **6** must have occurred through a $^1C_4$ *pseudo*-chair conformation of the 6-(oxytriphenylphosphonium) Mitsunobu intermediate **9**, even though this pyranose ring conformation is disfavored according to the NMR studies of **1** in methanol solution.

Both **5** and **6** were evaluated[13] for inhibitory activity against the SpHex *N*-acetylhexosaminidase and were found to be inactive.

2.5. Summary of GlcNAc-thiazoline conformations

Table 5 summarizes the important vicinal proton coupling constants and the observed conformations for the various GlcNAc-thiazolines presented herein. Fully O-acylated derivatives (**2** and

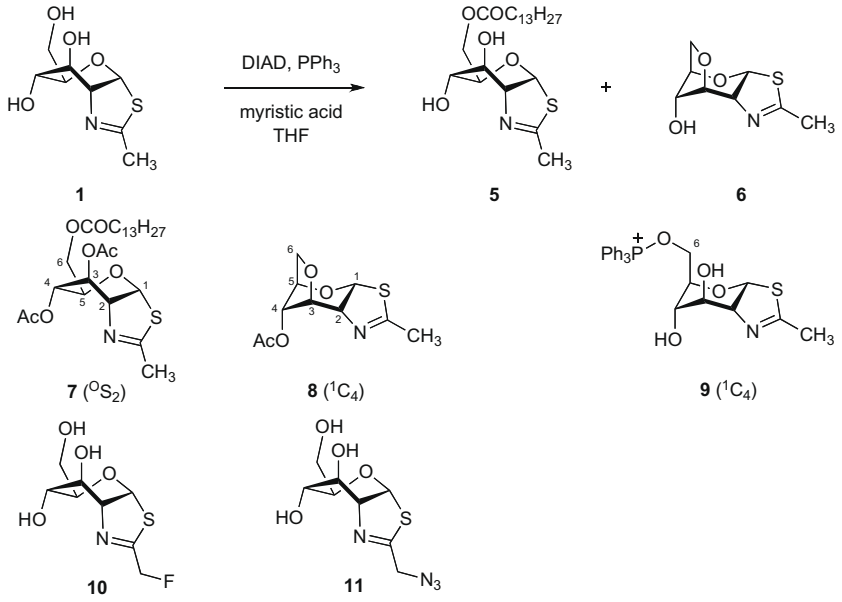

Scheme 1.

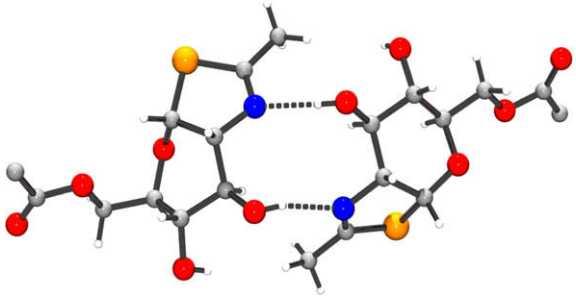

Figure 3. Crystal structure of the 6-*O*-tetradecanoate **5**, showing the two molecules in conformations $^{1}S_{3}$ (left) and $^{4}C_{1}$ (right) H-bonded to one another in the unit cell. The tetradecanoate chain has been truncated to acetate for clarity.

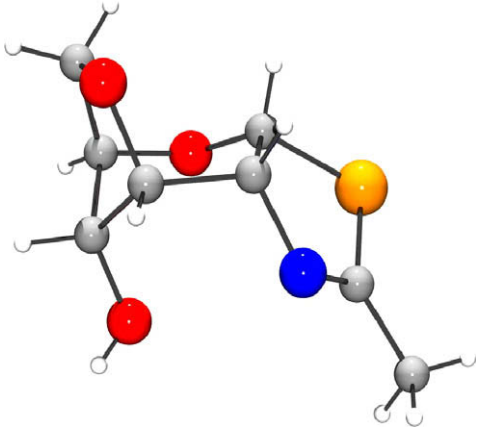

Figure 4. Crystal structure of the tricyclic thiazoline ether **6** in the bridge-enforced $^{1}C_{4}$ conformation.

7) in solution are best described as $^{O}S_{2}$ *pseudo*-(twist boats), a conformation also previously observed in solution and in the crystal for the corresponding 3,4,5-tri-*O*-acetyl-GlcNAc-*oxazoline*[16] as well as a variety of methyl-functionalized and O-acetylated GlcNAc-thiazoline analogues.[12] The triol **1** and also its mono-acyl derivative

Table 5
Vicinal coupling constants and conformations of GlcNAc-thiazolines[a]

Compound	$J_{1,2}$	$J_{2,3}$	$J_{3,4}$	$J_{4,5}$	Conform'n
1 (MeOH-d_4)	7.2	4.2	3.8	9.2	$^{O}S_{2}$, $^{4}C_{1}$, $^{1}S_{3}$
2 ($CDCl_3$)	7.2	3.1	1.7	9.2	$^{O}S_{2}$
5 (MeOH-d_4)	7.2	4.8	3.6	9.2	$^{O}S_{2}$ et al.
5 (Crystal)					$^{4}C_{1}$ and $^{1}S_{3}$
6 ($CDCl_3$)	4.8	4.8	4.8	3.0	$^{1}C_{4}$
6 (Crystal)					$^{1}C_{4}$
7 ($CDCl_3$)	7.2	3.0	1.5	9.3	$^{O}S_{2}$
8 ($CDCl_3$)	5.1	4.2	5.4	3.0	$^{1}C_{4}$
10 (MeOH-d_4)	7.2	4.4	4.0	9.2	$^{O}S_{2}$ et al.
11 (MeOH-d_4)	7.0	4.5	4.0	9.2	$^{O}S_{2}$ et al.

[a] Coupling constants in hertz.

5 in solution have mostly the $^{O}S_{2}$ conformation, with contributing minor conformations $^{4}C_{1}$ and $^{1}S_{3}$ mixed in. Since mono-acylation at O-6 does not effect the solution conformation, hydrogen bonding of the 6-OH must not play a major role determining the ring conformation. In the crystal, **5** is found as equal parts $^{4}C_{1}$ and $^{1}S_{3}$ hydrogen bonded to one another. Substitution of one of the methyl hydrogens of **1** by fluoro- or azido- has led to the respective inhibitory thiazolines **10** and **11**;[12] these have solution conformations that closely match those of **1**. The bridged pyranoses **6** and **8** in solution are constrained $^{1}C_{4}$ *pseudo*-chairs, as expected.

3. Conclusions

The *N*-acetylhexosaminidase inhibitor GlcNAc-thiazoline **1** is conformationally mobile in solution, existing simultaneously in a pyranose *pseudo*-chair and two *pseudo*-(twist boats)—$^{4}C_{1}$, $^{O}S_{2}$, and $^{1}S_{3}$, respectively—each detectable by NOE studies. The energy differences among them are likely on the order of 1–2 kcal/mol, according to calculations. Furthermore, a monoacyl derivative **5** crystallizes simultaneously in the $^{4}C_{1}$ and $^{1}S_{3}$ conformations, again suggesting a small energy difference. Because the energy differences among these three conformations are small, it is difficult to specify what factors control the conformation distribution, although 1,3-diaxial steric repulsions (C-6/O-2 and N/O-3) likely account for why the $^{1}C_{4}$ contributes little to the mix.

An implication of this work for enzyme inhibitor design is that flexible molecules resemble small libraries of inhibitor candidates. One conformation, not necessarily the most stable one, is certain to be superior to the others in terms of inhibition efficacy. Enzymes are thought to catalyze reactions by stabilizing the substrate-derived transition state.[17] The inhibitor **1** binds in the *N*-acetylhexosaminidase active site as the $^4C_1$ pseudo-chair, the conformation that most closely matches the substrate transition state (**B**, Fig. 1).

4. Experimental

4.1. (3a*R*,5*R*,6*S*,7*R*,7a*R*)-6,7-Dihydroxy-5-(tetradecanoyloxymethyl)2-methyl-5,6,7,7a-tetrahydro-3a*H*-pyrano[3,2-d]thiazole (5) and (3a*R*,5*R*,6*S*,7*R*,7a*R*)-7-Hydroxy-5,7-(methyleneoxy)-2-methyl-5,6,7,7a-tetrahydro-3a*H*-pyrano[3,2-d]thiazole (6)

Diisopropyl azodicarboxylate (118 μl, 0.60 mmol) was added to a stirred solution of 158 mg (0.60 mmol) of triphenylphosphine in 4 mL of THF while maintaining a bath temperature of −20 to −30 °C. After 30 min, a thick white precipitate had formed. The mixture was cooled with a −78 °C bath, and then a solution of 160 mg (0.70 mmol) of myristic acid in 2 mL of THF was added, followed by a solution of 44 mg of the thiazoline triol[2] **1** in 1 mL of THF. The reaction mixture was allowed to warm to 23 °C, and the resulting pale yellow solution was stirred for an additional 18 h. The reaction mixture was concentrated and then chromatographed on silica with ethyl acetate as the eluant to afford 21 mg (21%) of the tetradecanoate **5** as a colorless solid: mp 84–86 °C; R_f 0.51 (9:1 dichloromethane/methanol); ^{1}H NMR (400 MHz, CD_3OD) δ 6.31 (d, 1H, J = 7.2), 4.32 (dddd, 1H, J = 7.2, 4.8, 2.4, 1.2), 4.25 (dd, 1H, J = 12.0, 2.8), 4.18 (dd, 1H, J = 12.0, 6.8), 4.13 (dd, 1H, J = 4.8, 3.6), 3.56 (ddd, 1H, J = 9.2, 3.6, 0.8), 3.47 (ddd, 1H, J = 9.2, 6.8, 2.4), 2.32 (t, 2H, J = 7.2), 2.25 (d, 3H, J = 2.0), 1.60 (br quint, 2 H, J = 7.2), 1.22–1.36 (m, 20 H), 0.89 (t, 3H, J = 7.2); ^{13}C NMR (100 MHz, CD_3OD) δ 174.1, 169.4, 89.3, 79.5, 72.8, 72.5, 70.4, 63.9, 33.8, 31.9, 29.6, 29.6, 29.6, 29.5, 29.4, 29.3, 29.2, 29.0 24.9, 22.5, 19.4, 13.2; ESI-MS *m/z* 430 MH^+, 452 MNa^+, 881 M_2Na^+. Crystals suitable for diffraction studies were grown by slow diffusion of petroleum ether into a toluene solution of **5**.

The column wash (methanol) from the reaction described above was purified by preparative TLC on silica with 19:1 dichloromethane/methanol as the eluant to afford 4 mg (10%) of the cyclized anhydro product **6** as a colorless solid: mp 114–117 °C; R_f 0.45 (19:1 dichloromethane/methanol); ^{1}H NMR (300 MHz, $CDCl_3$) δ 5.93 (d, 1H, J = 4.8), 4.86 (t, 1H, J = 4.8); 4.29 (d, 1H, J = 11.1), 4.24 (br t, 1H, J = 3.0), 4.14–4.22 (m, 2H), 4.07 (dd, 1H, J = 11.1, 3.0), 2.45 (d, 1H, J = 9.0), 2.34 (d, 3H, J = 2.7); ^{13}C NMR (75 MHz, $CDCl_3$) δ 168.0, 85.9, 80.5, 76.9, 72.4, 71.9, 68.4, 20.9; ESI-MS *m/z* 202 MH^+. Crystals suitable for diffraction studies were grown by slow diffusion of petroleum ether into a toluene solution of **6**.

4.2. Acetate derivatives 7 and 8

Separate treatment of **5** and **6** with acetic anhydride in pyridine solution followed by column chromatography gave the respective acetate derivatives **7** and **8**. Data for **7**: ^{1}H NMR (300 MHz, $CDCl_3$) δ 6.24 (d, 1H, J = 7.2), 5.57 (dd, 1H, J = 3.0, 1.5), 4.95 (br d, 1H, J = 9.3), 4.44–4.50 (m, 1H), 4.15 (dd, 1H, J = 12.3, 3.3), 4.10 (dd, 1H, J = 12.3, 5.7), 3.54 (ddd, 1H, J = 9.0, 5.4, 3.3), 2.33 (t, 2H, J = 7.8), 2.32 (d, 3H, J = 2.4), 2.14 (s, 3H), 2.09 (s, 3H), 1.62 (br quint, 1H, J = 7.2), 1.22–1.34 (m, 20 H), 0.88 (t, 3H, J = 6.6); ^{13}C NMR (75 MHz, $CDCl_3$) δ 172.3, 168.4, 168.1, 167.0, 87.8, 75.7, 69.7, 68.3, 67.6, 62.1, 33.1, 31.0, 28.7, 28.7, 28.7, 28.7, 28.6, 28.4, 28.4, 28.2, 24.0, 21.8, 20.1, 20.0, 19.8, 13.2; ESI-MS *m/z* 536 MNa^+. Data for **8**: ^{1}H NMR (300 MHz, $CDCl_3$) δ 5.94 (d, 1H, J = 5.1), 5.12 (dd, 1H, J = 5.4, 4.2), 4.86 (br dd, 1H, J = 5.4, 3.3), 4.44 (br t, 1H, J = 3.0), 4.28 (d, 1H, J = 11.1), 4.20–4.28 (m, 1H), 4.07 (dd, 1H, J = 11.1, 3.3), 2.29 (d, 3H, J = 2.4), 2.06 (s, 3H); ^{13}C NMR (75 MHz, $CDCl_3$) δ 169.5, 163.1, 83.4, 79.5, 73.0, 70.6, 69.5, 67.4, 19.6, 19.4; ESI-MS *m/z* 244 MH^+, 266 MNa^+, 509 M_2Na^+.

4.3. NOE studies

NOESY1D spectra of **1** (see Supplementary data) were acquired on a solution of 18.9 mg in 0.75 mL of methanol-d_4 at 25 °C and 500 MHz. Coupling constants and NOE measurements were also evaluated at twofold and fourfold dilution, and were observed to be invariant.

4.4. Calculations

The GAUSSIAN 03 package[18] was used to carry out all calculations. Standard Pople-type basis sets were employed.[19] All geometries were optimized using hybrid density functional theory, the 6-31G* basis set, and the B3LYP functional.[20] All structures were verified as minima by the calculation of vibrational frequencies. Single point energies were calculated at B3LYP/6-311++G** using the B3LYP/6-31G* optimized geometries. Zero-point energies calculated at B3LYP/6-31G*, and corrected by a scale factor of 0.9804,[21] were included in the energies reported. Isotropic shielding values were computed using the GIAO method[22] in conjunction with the B3LYP/6-311++G**//B3LYP/6-31G* level of theory. This procedure, together with appropriate empirical scaling has been shown previously to provide proton chemical shifts with an accuracy of ±0.15 ppm.[23] The calculated proton isotropic shielding values were converted to chemical shifts by using the previously described scaling procedure. In the case of carbon, the calculated isotropic shielding values were converted to chemical shifts by using the average of all chemical shifts (and the average of all calculated isotropic shielding values) in the molecule as an internal standard according to: $\delta_i = (\delta_{avg} + \chi_{avg}) - \chi_i$. Spin–spin coupling constants were computed using the spinspin keyword.[24]

Acknowledgments

We thank NIH (AI055760) for partial financial support, the Henry Rutgers Honors Program at Rutgers for an undergraduate fellowship to DF, Rohm and Haas Co. for a graduate assistantship to MA, and Brian Rempel and Stephen G. Withers (UBC) for the enzymatic evaluation of **5** and **6**. PRR thanks the Henry Dreyfus Teacher-Scholar Awards Program administered by the Camille and Henry Dreyfus Foundation for partial support of this research at Swarthmore.

Supplementary data

Copies of NMR spectra for new compounds and NOE experiments, Cartesian coordinates and energies of the conformations of **1**, and CIFs and ORTEPs for **5** and **6**. Supplementary data associated with this article can be found, in the online version, at doi:10.1016/j.bmc.2009.01.066.

References and notes

1. (a) Tews, I.; Perrakis, A.; Oppenheim, A.; Dauter, Z.; Wilson, K. S.; Vorgias, C. E. *Nat. Struct. Biol.* **1996**, *3*, 638; (b) Tews, I.; Terwisscha van Scheltinga, A. C.; Perrakis, A.; Wilson, K. S.; Dijkstra, B. W. *J. Am. Chem. Soc.* **1997**, *119*, 7954; (c) Mark, B. L.; Wasney, G. A.; Salo, T. J.; Khan, A. R.; Cao, Z.; Robbins, P. W.; James, M. N. G.; Triggs-Raine, B. L. *J. Biol. Chem.* **1998**, *273*, 19618; (d) Drouillard, S.; Armand, S.; Davies, G. J.; Vorgias, C. E.; Henrissat, B. *Biochem. J.* **1997**, *328*, 945.
2. Knapp, S.; Vocadlo, D.; Gao, Z.; Kirk, B.; Lou, J.; Withers, S. G. *J. Am. Chem. Soc.* **1996**, *118*, 6804.

3. Mark, B. L.; Vocadlo, D. J.; Knapp, S.; Triggs-Raine, B. L.; Withers, S. G.; James, M. N. G. *J. Biol. Chem.* **2001**, *276*, 10330.
4. Macauley, M. S.; Whitworth, G. E.; Debowski, A. W.; Chen, D.; Vocadlo, D. J. *J. Biol. Chem.* **2005**, *280*, 25313.
5. Whitworth, G. E.; Macauley, M. S.; Stubbs, K. A.; Dennis, R. J.; Taylor, E. J.; Davies, G. J.; Greig, I. R.; Vocadlo, D. J. *J. Am. Chem. Soc.* **2007**, *129*, 635.
6. Dennis, R. J.; Taylor, E. J.; Macauley, M. S.; Stubbs, K. A.; Turkenburg, J. P.; Hart, S. J.; Black, G. N.; Vocadlo, D. J.; Davies, G. J. *Nat. Struct. Mol. Biol.* **2006**, *13*, 365.
7. Mark, B. L.; Mahuran, D. J.; Cherney, M. M.; Zhao, D.; Knapp, S.; James, M. N. G. *J. Mol. Biol.* **2003**, *327*, 1093.
8. Maier, T.; Strater, N.; Schuette, C. G.; Klingenstein, R.; Sandhoff, K.; Saenger, W. *J. Mol. Biol.* **2003**, *328*, 669.
9. Langley, D. B.; Harty, D. W. S.; Jacques, N. A.; Hunter, N.; Guss, J. M.; Collyer, C. A. *J. Mol. Biol.* **2008**, *377*, 104.
10. See discussion in: Silverman, R. B. *The Organic Chemistry of Drug Design and Drug Action*, 2nd ed.; Elsevier Academic Press: Amsterdam, The Netherlands, 2004. pp 152–172.
11. For a discussion in the area of HIV inhibition, see: Das, K.; Lewi, P. J.; Hughes, S. H.; Arnold, E. *Prog. Biophys. Mol. Biol.* **2005**, *88*, 209.
12. Knapp, S.; Abdo, M.; Ajayi, K.; Huhn, R. A.; Emge, T. J.; Kim, E. J.; Hanover, J. A. *Org. Lett.* **2007**, *9*, 2321.
13. Amorelli, B.; Yang, C.; Rempel, B.; Withers, S. G.; Knapp, S. *Bioorg. Med. Chem. Lett.* **2008**, *18*, 2944.
14. The NOEs observed for **1** are assumed to be largely intramolecular rather than intermolecular because they are acquired in methanol-d_4 solution. This solvent, which is a strong hydrogen bond donor, is present in 214-fold molar excess. An H-bonded dimer of **1** featuring N···HO(3) hydrogen bonds (as in Fig. 3) in solution might contribute a long range intermolecular (as little as ~2.6 Å, as estimated from the crystal structure) H(3)···CH_3' contact, which in turn might result in an NOE crosspeak. The very weak H(3)···CH_3 crosspeak observed for **1** (Table 3) might represent a minor contribution from this dimer. However, this crosspeak persisted without variation upon two- and fourfold dilution, consistent with an intramolecular through-space contact.
15. For each of the four major conformations $^{O}S_2$, $^{4}C_1$, $^{1}S_3$, and $^{1}C_4$, the three possible rotamers about the C_5–C_6 bond were separately considered, and the lowest energy conformer selected for further analysis.
16. Foces-Foces, C.; Cano, F. H.; Bernabe, M.; Penades, S.; Martin-Lomas, M. *Carbohydr. Res.* **1984**, *135*, 1.
17. Pauling, L. *Nature* **1948**, *161*, 707.
18. Frisch, M. J.; Trucks, G. W.; Schlegel, H. B.; Scuseria, G. E.; Robb, M. A.; Cheeseman, J. R.; Montgomery, Jr., J. A.; Vreven, T.; Kudin, K. N.; Burant, J. C.; Millam, J. M.; Iyengar, S. S.; Tomasi, J.; Barone, V.; Mennucci, B.; Cossi, M.; Scalmani, G.; Rega, N.; Petersson, G. A.; Nakatsuji, H.; Hada, M.; Ehara, M.; Toyota, K.; Fukuda, R.; Hasegawa, J.; Ishida, M.; Nakajima, T.; Honda, Y.; Kitao, O.; Nakai, H.; Klene, M.; Li, X.; Knox, J. E.; Hratchian, H. P.; Cross, J. B.; Bakken, V.; Adamo, C.; Jaramillo, J.; Gomperts, R.; Stratmann, R. E.; Yazyev, O.; Austin, A. J.; Cammi, R.; Pomelli, C.; Ochterski, J. W.; Ayala, P. Y.; Morokuma, K.; Voth, G. A.; Salvador, P.; Dannenberg, J. J.; Zakrzewski, V. G.; Dapprich, S.; Daniels, A. D.; Strain, M. C.; Farkas, O.; Malick, D. K.; Rabuck, A. D.; Raghavachari, K.; Foresman, J. B.; Ortiz, J. V.; Cui, Q.; Baboul, A. G.; Clifford, S.; Cioslowski, J.; Stefanov, B. B.; Liu, G.; Liashenko, A.; Piskorz, P.; Komaromi, I.; Martin, R. L.; Fox, D. J.; Keith, T.; Al-Laham, M. A.; Peng, C. Y.; Nanayakkara, A.; Challacombe, M.; Gill, P. M. W.; Johnson, B.; Chen, W.; Wong, M. W.; Gonzalez, C.; and Pople, J. A.; Gaussian 03, Revision C.02: Gaussian, Inc., Wallingford CT, 2004.
19. Hehre, W. J.; Radom, L.; Schleyer, P. v. R.; Pople, J. A. *Ab Initio Molecular Orbital Theory*; Wiley: New York, 1986.
20. (a) Becke, A. D. *J. Chem. Phys.* **1993**, *98*, 5648; (b) Lee, C.; Yang, W.; Parr, R. G. *Phys. Rev. B* **1988**, *37*, 785; (c) Miehlich, B.; Savin, A.; Stoll, H.; Preuss, H. *Chem. Phys. Lett.* **1989**, *157*, 200.
21. Foresman, J. B.; Frisch, A. *Exploring Chemistry with Electronic Structure Methods*; Gaussian: Pittsburgh, 1996.
22. (a) London, F. *J. Phys. Radium* **1937**, *8*, 397; (b) Ditchfield, R. *Mol. Phys.* **1974**, *27*, 789; (c) Wolinski, K.; Hilton, J. F.; Pulay, P. *J. Am. Chem. Soc.* **1990**, *112*, 8251.
23. Rablen, P. R.; Pearlman, S. A.; Finkbiner, J. *J. Phys. Chem. A* **1999**, *103*, 7357.
24. (a) Helgaker, T.; Watson, M.; Handy, N. C. *J. Chem. Phys.* **2000**, *113*, 9402; (b) Sychrovsky, V.; Gräfenstein, J.; Cremer, D. *J. Chem. Phys.* **2000**, *113*, 3530; (c) Barone, V.; Peralta, J. E.; Contreras, R. H.; Snyder, J. P. *J. Phys. Chem. A* **2002**, *106*, 5607.